Colloidal Sedimentation in Polymer Solutions

X. Ye[†] and P. Tong*

Department of Physics, Oklahoma State University, Stillwater, Oklahoma 74078

L. J. Fetters

Exxon Research and Engineering Company, Route 22 East, Annandale, New Jersey 08801

Received December 30, 1997; Revised Manuscript Received July 11, 1998

ABSTRACT: We report sedimentation measurements of small colloidal particles through a nonadsorbing polymer solution. The particle sedimentation velocity $v_c(\phi_c,C_p)$, as a function of the colloid volume fraction ϕ_c and the polymer concentration C_p, is found to be affected by both the microscopic viscosity $\eta_c(C_p)$ experienced by the particles in the solution and the polymer-induced depletion interaction between the particles. The measurements reveal a large effect of the depletion interaction on colloidal sedimentation in the high-ϕ_c samples. The experiment demonstrates the effectiveness of using the sedimentation method to study interaction-related phenomena in colloidal suspensions.

1. Introduction

The study of the transport of macromolecules in a spatially inhomogeneous medium, such as a polymer gel or a porous medium, is of fundamental interest in statistical physics and is also relevant to many technological and biological processes involving separating or removing polymer molecules, proteins, and other large biomolecules.[1] To understand the transport phenomena in a complex medium, one needs to know the local conformation of the macromolecules being transported, the characteristics of the spatial inhomogeneity of the medium, and the interactions between the macromolecules and the medium. In this paper, we consider a simple case of sedimentation of a suspension of colloidal particles through a nonadsorbing polymer solution, in which the polymer chains form a fluctuating network.[2] The colloidal particle chosen for the study consists of a calcium carbonate core stabilized by a monolayer of surfactant molecules. The polymer used is hydrogenated polyisoprene, a stable straight-chain polymer. Both the colloid and the polymer are dispersed in a good solvent, decane, and their solution properties have been well-characterized previously by using various experimental techniques. Such a nonaqueous colloid−polymer mixture system is ideal for the investigation attempted here, because the shape of the particles is simple and remains unchanged during sedimentation. The spatial structure of semidilute polymer solutions has been intensively studied for many years and now is well-understood.[2]

The main issue in colloidal sedimentation is to understand how particle−particle and particle−polymer interactions affect the particle sedimentation velocity $v_c(\phi_c,C_p)$ as a function of the colloid volume fraction ϕ_c and the polymer concentration C_p.[3,4] (Hereafter, we will use the subscripts c and p to refer to the colloid and polymer, respectively.) The free polymer molecules in the colloidal suspension can affect $v_c(\phi_c,C_p)$ in two different ways. For a sufficiently dilute colloidal suspension, the separation between the particles is so large that their interaction can be ignored. In this case, adding polymer into the suspension increases the viscosity of the solution, and therefore the colloidal particles will experience a larger frictional force [i.e., $v_c(\phi_c,C_p)$ is reduced]. For a concentrated colloid−polymer mixture, however, the interaction potential $U(r)$ between the particles can develop an attractive well because the polymer chains are expelled from the region between two particles when their surface separation becomes smaller than the size of a polymer chain.[5,6] This depletion attraction will change the spatial configuration of the particles in the solution and increase their sedimentation velocity $v_c(\phi_c,C_p)$.

Recently, we have conducted a sedimentation study of a dilute suspension of colloidal particles through a nonadsorbing polymer solution.[7] In the experiment, we measured the viscosity ratio η_c/η_0, where η_c is the microscopic viscosity experienced by the particles in the polymer solution and η_0 is the solvent viscosity. The experiment reveals that when the particle's hydrodynamic radius R_h is smaller than the polymer correlation length ξ, which describes the average mesh size of the fluctuating polymer network, the particles "feel" the linear viscosity of the solution rather than the solvent viscosity η_0. The measured viscosity ratio is found to have the form $\eta_c/\eta_0 = 1 + [\eta]C_p$, where $[\eta]$ is the intrinsic viscosity of the polymer solution. When $R_h \gg \xi$, the particles experience the macroscopic viscosity η_p of the polymer solution, as suggested by de Gennes et al.[2,8] In this case, the measured η_c/η_0 is found to be equal to $\eta_p/\eta_0 = 1 + [\eta]C_p + k_H([\eta]C_p)^2$, with k_H being the Huggins coefficient. In the transition region, the measured η_c/η_0 does not have the predicted scaling form $\varphi(R_h/\xi)$.[8] Instead, a new switch function, $S_c(C_p) \equiv [\eta_c/\eta_0 - (1 + [\eta]C_p)]/[k_H([\eta]C_p)^2]$, is found to be of universal form independent of the polymer molecular weight M_p.[7]

In this paper, we report sedimentation measurements of the concentrated colloidal particles through a nonadsorbing polymer solution, in which the polymer-induced depletion interaction becomes important. We have recently studied the depletion interaction in the colloid−polymer mixture using the small-angle neutron scattering (SANS) technique.[9,10] By matching the scat-

* To whom correspondence should be addressed. E-mail: ptong@osuunx.ucc.okstate.edu.

[†] Also at Department of Physics, Northeastern University, Shenyang, People's Republic of China.

S0024-9297(97)01892-5 CCC: $15.00
Published on Web 08/25/1998

tering length density of the solvent with that of the polymer, we measured the colloid partial structure factor $S_c(Q)$ over a suitable range of the scattering wavenumber Q. It was found that the measured $S_c(Q)$ can be well-described by the depletion potential $U(r)$. With the measured interaction parameters, we can vary the depletion attraction systematically and study the effect of the thermodynamic interaction on $v_c(\phi_c,C_p)$ in great detail. Once the interaction effect is understood, one can in turn use the sedimentation method to measure the particle interaction in different colloidal systems.

The paper is organized as follows. In section 2, we review the thermodynamic theory for the depletion potential $U(r)$ and calculate its effect on $v_c(\phi_c,C_p)$. Experimental details appear in section 3, and the results are discussed in section 4. Finally, the work is summarized in section 5.

2. Theoretical Background

As mentioned in section 1, the addition of free polymer molecules into a colloidal suspension can have two competing effects on $v_c(\phi_c,C_p)$. It can either reduce $v_c(\phi_c,C_p)$ because the solution viscosity is increased or increase $v_c(\phi_c,C_p)$ because of the depletion attraction between the particles. Experimentally, one can separate the two effects by changing the colloid concentration ϕ_c. For a dilute colloidal suspension, the particle interaction can be ignored and $v_c(\phi_c,C_p)$ becomes the Stokes velocity,

$$v_s(C_p) = \frac{2R_h^2 \Delta d A}{9\eta_c(C_p)} \tag{1}$$

which is determined by the balance between the centripetal force and the viscous drag. In the above, A is the centripetal acceleration, Δd is the density difference between the solvent and the particle, and $\eta_c(C_p)$ is the microscopic viscosity experienced by the particles in the polymer solution at the concentration C_p.

For a concentrated colloidal suspension, the interparticle hydrodynamic interaction created by the motion of the surrounding particles introduces a correction to the Stokes velocity $v_s(C_p)$.[3,11] It has been shown that $v_c(\phi_c,C_p)$ can be written as[11]

$$v_c(\phi_c,C_p) = v_s(C_p)\, f(\phi_c;U) \tag{2}$$

where the hindered settling function $f(\phi_c;U)$ is a decreasing function of ϕ_c with $f(0;0) = 1$. Note that $f(\phi_c;U)$ also depends on the thermodynamic interaction potential $U(r)$ between the particles. For a repulsive colloidal system, $U(r)$ tends to keep the particles well-separated and $f(\phi_c;U)$ is reduced because of the back flow of the solvent produced by the falling particles. For an attractive colloidal system, on the other hand, $U(r)$ creates an excess of particles surrounding a test particle. The drag coefficient of these temporary particle clusters is smaller than that of a uniform suspension, and hence $f(\phi_c;U)$ is increased.[11]

In a mixture of a colloid and a nonadsorbing polymer, $f(\phi_c;U)$ changes with the polymer concentration C_p through the depletion potential[6,10]

$$U(r) = \begin{cases} +\infty & r \le \sigma \\ -\Pi_p(C_p)\, V_0(r) & \sigma < r \le \sigma + 2R_g \\ 0 & r > \sigma + 2R_g \end{cases} \tag{3}$$

where σ is the particle diameter, $\Pi_p(C_p)$ is the osmotic pressure of the polymer molecules, and R_g is their radius of gyration. The volume $V_0(r)$ of the overlapping depletion zones between the two particles at a separation r is given by[6,10]

$$V_0(r) = \tilde{v}_p\left(\frac{\lambda}{\lambda - 1}\right)^3\left[1 - \frac{3}{2}\left(\frac{r}{\sigma\lambda}\right) + \frac{1}{2}\left(\frac{r}{\sigma\lambda}\right)^3\right] \tag{4}$$

where $\tilde{v}_p = (4\pi/3)R_g^3$ is the volume occupied by a polymer chain and $\lambda = 1 + 2R_g/\sigma$. In the above, we have assumed that the colloidal particles are hard spheres in the absence of the free polymer chains. Our recent neutron scattering experiment has shown[9,10] that, for the colloid−polymer system used in the present study, the measured colloidal structure factor $S_c(Q)$ can indeed be described by the potential $U(r)$ in eq 3.

Because of the complexities of the many-body hydrodynamic interaction in sedimentation, the exact functional form of $f(\phi_c;U)$ is not known at the moment.[3,11] For low colloid concentrations, however, Batchelor[12] has shown that

$$f(\phi_c;U) \simeq 1 - \phi_c\left[5 + 3\int_2^{+\infty} dx\, x[1 - g(x)] + \frac{15}{4}\int_2^{+\infty} dx\, \frac{g(x)}{x^2}\right] \tag{5}$$

where $x = 2r/\sigma$ and the pair distribution function $g(r) = \exp[-U(r)/(k_BT)]$. Because $U(r)$ in eq 3 consists of a hard-sphere potential plus an attractive well $U_d(r) = -\Pi_p(C_p)\, V_0(r)$, eq 5 can be rewritten as

$$f(\phi_c;U) \simeq 1 - (K_c + K_p)\phi_c \tag{6}$$

where

$$K_c = 5 + \frac{15}{4}\int_2^{+\infty} dx\, \frac{1}{x^2} \tag{7}$$

$$K_p = \int_2^{2\lambda} dx \left(\frac{15}{4x^2} - 3x\right)\left(e^{-U_d(x)/k_BT} - 1\right) \tag{8}$$

In the above, K_c represents the contribution from the hard spheres and K_p is due to the polymer-induced depletion interaction and thus depends on C_p.

With eq 7 we have $K_c = 6.875$. When higher orders of the hydrodynamic interaction are included, Batchelor[12] found $K_c = 6.55$ for monodisperse hard spheres suspended uniformly in a solution at thermal equilibrium. Under these conditions, one has

$$f(\phi_c;U) \simeq 1 - K_c\phi_c \simeq (1 - \phi_c)^{K_c} \tag{9}$$

where the last equality is an empirical result, which can describe the sedimentation data over a wider range of ϕ_c.[3] In several well-characterized colloidal suspensions, Batchelor's prediction has been confirmed.[3,13,14] When $U_d(r)/k_BT$ is small, one can expand the exponential function in eq 8 and obtain an analytic form for K_p. With eqs 3, 4, and 8 we find [up to the first order of $U_d(x)/k_BT$]

$$K_p = \tilde{P}(C_p)\left(\frac{\lambda}{\lambda - 1}\right)^3\left(-\frac{6}{5}\lambda^2 + \frac{63}{8} - \frac{45\ln\lambda}{16\lambda} - \frac{237}{32}\frac{1}{\lambda} + \frac{117}{160}\frac{1}{\lambda^3}\right) \tag{10}$$

where the interaction amplitude $\tilde{P}(C_p) = \Pi_p(C_p)\nu_p/k_BT$. In a recent neutron scattering experiment,[9,10] we measured $\tilde{P}$ as a function of C_p. The value of λ was also obtained in the experiment.

It is seen from eq 8 that K_p contains the same probability factor, $\exp[-U_d(x)/k_BT] - 1$, as the second virial coefficient A_2 does in thermodynamics. The only difference between the two coefficients is that the probability factor in eq 8 is averaged over a different weighting factor (the two-body mobility function). The coefficient A_2 can be obtained from the concentration dependence of the scattered light intensity measured at the small-angle limit $Q \rightarrow 0^+$. With the virial expansion for the structure factor $S_c(Q=0)$, one has[15]

$$\frac{1}{S_c(0)} \simeq 1 + 2\frac{A_2}{\tilde{\nu}_c}\phi_c \tag{11}$$

where $\tilde{\nu}_c = (\pi/6)\sigma^3$ is the volume of the particle and

$$A_2 = 2\pi\int_0^\infty (1 - e^{-U(r)/k_BT})r^2\, dr \tag{12}$$

Using the potential $U(r)$ in eq 3, we find $A_2/\tilde{\nu}_c = B_c + B_p$ with $B_c = 4$ and

$$B_p = \int_2^{2\lambda} dx \left(\frac{-3x^2}{2}\right)(e^{-U_d(x)/k_BT} - 1) = \tilde{P}(C_p)\left(\frac{\lambda}{\lambda - 1}\right)^3\left(4 - \frac{\lambda^3}{2} - \frac{9}{2\lambda} + \frac{1}{\lambda^3}\right) \tag{13}$$

Clearly, the thermodynamic parameter B_p plays a role similar to that of K_p in sedimentation.

3. Experimental Methods

The colloid−polymer system chosen for the study has been well-characterized previously and has been detailed elsewhere.[10] Here we only mention a few key points. The colloidal particle consists of a calcium carbonate ($CaCO_3$) core with an adsorbed monolayer of a randomly branched calcium alkylbenzenesulfonate surfactant. The average density of the particle is $d_c \simeq 2.0$ g/cm.[3] The colloidal samples are prepared by diluting known amounts of the concentrated suspension with the solvent, decane. The resulting suspension is found to be relatively monodispersed with an average hydrodynamic radius $R_h = 5$ nm and ~10% standard deviation.[15] Our recent small-angle scattering measurements[10] revealed that the particle has a core radius of $R_0 = 2.0$ nm and a surfactant monolayer thickness of $\delta = 2.0$ nm. Thus the static (or mass) radius of the particle is $R_m = R_0 + \delta = 4.0$ nm. Measurements of the particle structure factor $S_c(Q)$ have shown that the colloidal suspension behaves like a hard-sphere system.[9,10] By fitting the measured $S_c(Q)$ with the hard-sphere model, we obtained the colloid volume fraction ϕ_c of the scattering samples. These values of ϕ_c and their linear extrapolations are used in the present experiment to indicate the colloid concentration of the sedimentation samples.

The polymer used in the experiment is hydrogenated polyisoprene (poly(ethylene-propylene) or PEP), a straight-chain polymer synthesized by an anionic polymerization scheme.[16,17] The PEP is a model polymer ($M_w/M_n < 1.1$) and has been well-characterized previously using various experimental techniques.[16−18] Decane is used as the solvent because it is a good solvent for both the colloid and the polymer. The density of decane is $d_s = 0.73$ g/cm^3 and its viscosity $\eta_0 = 0.838$ cP at 25 °C. Our recent scattering experiments[15,19] revealed that the PEP chains do not adsorb onto the colloidal surfaces. Using a capillary viscometer, Davidson et al.[18] have measured the viscosity of the polymer solution as a function of C_p (g/cm^3). They found that the ratio of the solution viscosity η_p to the solvent viscosity η_0 can be well-described by

$$\eta_p/\eta_0 = 1 + [\eta]C_p + k_H([\eta]C_p)^2 \tag{14}$$

where $[\eta] = 2.05 \times 10^{-2}M_p^{0.73}$ cm^3/g and $k_H = 0.35$.

Because the colloidal particles are very small, their sedimentation under the earth gravity is unobservable. To increase the settling velocity of the particles, we conducted centrifugation measurements using a Beckman L8-70M ultracentrifuge with a SW-40TI swinging bucket rotor. The capacity of the sample cells is 14 × 95 mm (diameter × height). The distance between the middle height of the cell and the rotation axis is $\bar{r} = 11.3$ cm. The colloidal samples were centrifuged at a rotation rate $f = 35\,000$ rpm for 4−12 h, depending on the sample viscosity. The corresponding centripetal acceleration $A = (2\pi f)^2\bar{r} \simeq 1.5 \times 10^8$ cm/s^2 [$(1.5 \times 10^5)g$], which is large enough to cause the particles to settle 1−5 cm toward the bottom of the cell. After the centrifugation, a sharp interface can be observed by eye in the initially uniform solution. This interface separates the upper clear solvent region from the lower dark-brown colloid-rich region. The traveling distance h of the interface was measured by a low-magnification microscope, which was mounted on a vertical translation stage controlled by a micrometer. Because of the size polydispersity and the concentration gradient of the particles, the sedimentation interface between the solvent and the bulk suspension has a finite width. A typical value of the interface width is 0.5 mm, which is less than 5% of the total traveling distance h. The particle settling velocity is obtained via $v_c(\phi_c,C_p) = h/t$, where t is the centrifugation time. By varying the rotation rate f and the centrifugation time t, we have verified that the traveling distance h goes as f^2t, which is expected. In the experiment we measured $v_c(\phi_c,C_p)$ for different values of ϕ_c and C_p. All the measurements were conducted at 22 °C. To reduce systematic errors in the experiment, we present the sedimentation data in terms of the velocity ratio, say, $v_c(\phi_c,0)/v_c(\phi_c,C_p)$. In this way, all the system-dependent parameters are canceled out.

It should be pointed out that while the effective colloid concentration increases during the centrifugation, this increase does not affect the measured $v_c(\phi_c,C_p)$. This is because the concentration increase takes place only at the bottom of the sample cell, whereas $v_c(\phi_c,C_p)$ is determined by the position of the sedimentation interface, which is far away from the bottom of the cell. To verify this argument, we measured $v_c(\phi_c,C_p)$ at the same rotation rate ($f = 35\,000$ rpm) but with a different centrifugation time t. The traveling distance h of the interface (and hence the effective colloid concentration) is changed from 1 to 5 cm, but the final sedimentation velocity $v_c(\phi_c,C_p) = h/t$ is found to be the same. [For samples with a colloid concentration higher than 0.26 (which is beyond the concentration range of the present experiment), the particle interactions could produce a nonlinear t-dependence for $h(t)$.[3]] For the sedimentation measurements to be described below, the running time t is chosen such that h is in the range between 1 and 2 cm. Under this condition, the measured h is large enough so that the experimental uncertainties for $v_c(\phi_c,C_p)$ are small ($\delta h/h < 5\%$), and at the same time the change of the colloid concentration during the centrifugation is minimal (≃1 cm/ 9 cm).

Because the polymer density ($d_p = 0.856$ g/cm^3) is fairly close to that of decane ($d_s = 0.73$ g/cm^3), sedimentation of the polymer molecules during the centrifugation is negligible. To check the polymer sedimentation, we shine a He−Ne laser beam through the polymer sample with the beam direction normal to the fluid interface. If the polymer molecules in the solution settled, the upper phase (no polymer) will scatter much less light than the lower phase (more polymer) does, and therefore one should observe an abrupt intensity change along the scattering laser beam. Indeed, we observed this effect in a pure colloidal sample, in which a sharp sedimentation interface could also be seen by eye. For a polymer sample with $M_p = 1 \times 10^6$ (not used in the experiment), we did find such an abrupt intensity change along the scattering laser beam.

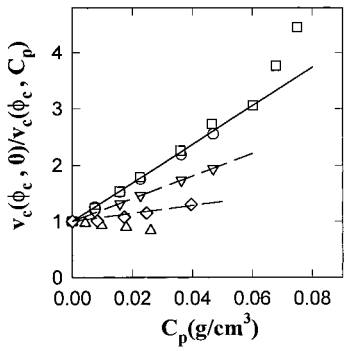

Figure 1. Measured $v_c(\phi_c,0)/v_c(\phi_c,C_p)$ as a function of C_p for the mixture samples with $\phi_c = 0.014$ (squares), 0.02 (circles), 0.041 (inverted triangles), 0.087 (diamonds), and 0.146 (triangles). The molecular weight of the PEP is $M_p = 26\,000$. The solid line shows the linear viscosity of the polymer solution, and the dashed lines are the linear fits to the data.

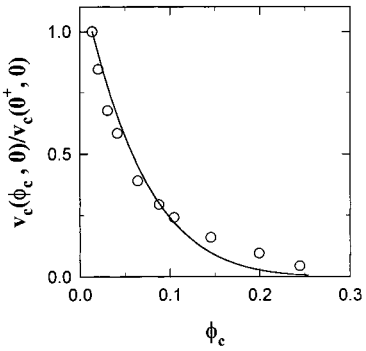

Figure 2. Measured $v_c(\phi_c,0)/v_c(0^+,0)$ as a function of ϕ_c for the pure colloidal sample. The solid curve is a plot of eq 15 for a hard-sphere system.

For all the polymer samples used in this experiment, however, we did not observe any abrupt intensity change along the scattering beam, indicating that no appreciable amount of sedimentation has occurred in these low molecular weight samples.

4. Results and Discussion

Figure 1 shows the measured $v_c(\phi_c,0)/v_c(\phi_c,C_p)$ as a function of C_p for the mixture samples with $\phi_c = 0.014$ (squares), 0.02 (circles), 0.041 (inverted triangles), 0.087 (diamonds), and 0.146 (triangles). The molecular weight of the PEP is $M_p = 26\,000$. In these samples, $\phi_c = 0.014$ is the lowest colloid concentration, at which one can still observe the sedimentation interface visually. It is seen from Figure 1 that the measured $v_c(\phi_c,0)/v_c(\phi_c,C_p)$ for the two samples with the lowest ϕ_c overlaps with each other, indicating that the system has reached the dilute limit and hence the particle interaction can be ignored in the sample with $\phi_c = 0.014$. From eqs 1 and 2 one finds that, in the dilute limit, $v_c(0^+,0)/v_c(0^+,C_p) = \eta_c/\eta_0$. Here we use the symbol 0^+ to indicate the dilute limit $\phi_c = 0.014$. Figure 1 shows that the measured η_c/η_0 for the $\phi_c = 0.014$ sample (squares) first increases linearly with C_p up to a value of $\tilde{C}_p \simeq 0.07$ g/cm^3 and then it turns up sharply. The solid line shows the linear viscosity, $1 + [\eta]C_p$, of the polymer solution measured independently by Davidson et al. (see eq 14). At even higher polymer concentrations, the measured η_c/η_0 (not shown in Figure 1) approaches the solution viscosity $\eta_p/\eta_0 = 1 + [\eta]C_p + k_H([\eta]C_p)^2$. Similar behavior of η_c/η_0 was also observed for the PEP with other molecular weights.[7]

It has been shown[7] that at the crossover concentration $\tilde{C}_p$, the correlation length ξ of the polymer solution becomes comparable to the hydrodynamic radius R_h of the particles. The measured η_c/η_0 in Figure 1 thus suggests that the particles "feel" the linear viscosity of the polymer solution when $C_p < \tilde{C}_p$, or equivalently, when $R_h < \xi$. Note that increasing C_p in the experiment is equivalent to reducing the value of ξ, because ξ is a decreasing function of C_p. Because the polymer concentration of the high-ϕ_c samples is all limited below $\tilde{C}_p$, the particles in these samples can only sense the linear viscosity of the solution. The polymer concentration of these samples could not be further increased because of the occurrence of phase separation induced by the depletion attraction. The measured $v_c(\phi_c,0)/v_c(\phi_c,C_p)$ as a function of C_p in the high-ϕ_c samples is found to decrease with increasing ϕ_c, indicating that the depletion attraction in these samples indeed gives rise to an increase in $v_c(\phi_c,C_p)$. In fact, the measured $v_c(\phi_c,0)/v_c(\phi_c,C_p)$ even starts to decrease with increasing C_p for the sample with the highest ϕ_c. This suggests that the effect of the depletion attraction due to the addition of the PEP polymer has overcome the effect of increasing viscosity. It is shown in Figure 1 that the measured $v_c(\phi_c,0)/v_c(\phi_c,C_p)$ is a linear function of C_p and the slope decreases when ϕ_c is increased (the dashed lines).

We now examine how the measured $v_c(\phi_c,C_p)$ changes with ϕ_c at a fixed C_p. We first discuss the measurements of the pure colloidal sample ($C_p = 0$). Figure 2 shows the measured $v_c(\phi_c,0)/v_c(0^+,0)$ as a function of ϕ_c. Because the particle is made of a $CaCO_3$ core plus a surfactant shell, its average mass density [and hence its Stokes velocity $v_c(0,0)$] is not accurately known. Therefore, we normalize the measured $v_c(\phi_c,0)$ with its low concentration limit $v_c(0^+,0)$. In this way, one can further reduce systematic errors in the experiment. From eq 2 one finds that the measured $v_c(\phi_c,0)/v_c(0^+,0)$ is proportional to $f(\phi_c;U)$, which reflects only the effect of the hydrodynamic interaction on sedimentation. It is seen from Figure 2 that the measured $v_c(\phi_c,0)/v_c(0^+,0)$ decays rapidly with ϕ_c. To compare the data with the hard-sphere calculation in eq 9, one needs to find out a particle radius and the corresponding volume fraction relevant to sedimentation. We have measured three different radii for the surfactant stabilized $CaCO_3$ particle. They are the hydrodynamic radius R_h (5.0 nm), the static mass radius R_m (4.0 nm), and the effective hard-sphere radius R_s (3.85 nm). These three radii were obtained, respectively, from a diffusion coefficient measurement, a static form factor measurement, and an interparticle structure factor measurement.[10,15] Because the surfactant shell of the particle is "soft", we expect R_s to be smaller than R_m. When the particle moves, its outer surfactant layer carries nearby solvent molecules along with it. Therefore, R_h should be larger than R_m. The volume fraction ϕ_c used in Figure 2 was obtained from the measurement of the interparticle structure factor, and hence it corresponds to R_s.

In sedimentation the relevant particle radius is R_h, and thus we find from eq 9 that

$$\frac{v_c(\phi_c,0)}{v_c(0^+,0)} = \left[\frac{1 - (R_h/R_s)^3\phi_c}{1 - 0.014(R_h/R_s)^3}\right]^{6.55} \qquad (15)$$

where $R_h/R_s = 1.3$ is the measured value for our particle. The solid curve in Figure 2 is a plot of eq 15 without any adjustable parameters. It is seen that the hard-sphere model fits the data satisfactorily for small values of ϕ_c up to $\phi_c = 0.1$. At higher colloid concentrations,

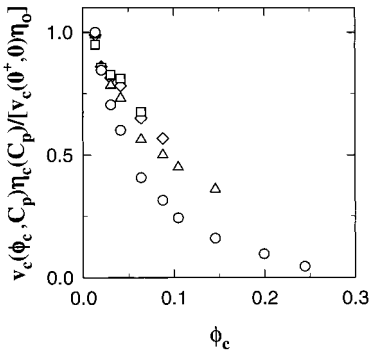

Figure 3. Measured $v_c(\phi_c,C_p)\ \eta_c(C_p)/[v_c(0^+,0)\eta_0]$ as a function of ϕ_c for the mixture samples with $C_p = 0$ (circles), 0.024 (triangles), 0.037 (diamonds), and 0.049 g/cm^3 (squares). The molecular weight of the PEP is $M_p = 26\,000$.

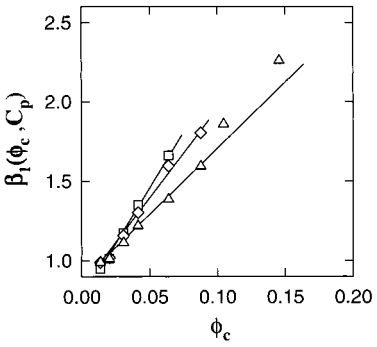

Figure 4. Plots of $\beta_1(\phi_c,C_p)$ as a function of ϕ_c for the mixture samples with $C_p = 0.024$ (triangles), 0.037 (diamonds), and 0.049 g/cm^3 (squares). The solid lines are the linear fits to the data.

the data show small deviations from the hard-sphere model. It should be pointed out that while the colloidal suspension behaves like a hard-sphere system thermodynamically, we do not expect that the particles act exactly as hard spheres hydrodynamically. Because of the surfactant corona around the particles, the flow boundary conditions for these particles are not the same as those for the hard spheres. Therefore, the short-range hydrodynamic interaction between the particles is changed. Consequently, $v_c(\phi_c,0)$ will be modified at higher colloid concentrations (i.e., at smaller interparticle distances).

Figure 3 shows how the measured $v_c(\phi_c,C_p)$ changes when PEP is added into the colloidal suspension. To eliminate the effect of the viscosity increase due to the addition of polymer, we normalize the measured $v_c(\phi_c,C_p)$ with $v_c(0^+,0)\eta_0/\eta_c(C_p)$, where $\eta_c(C_p)/\eta_0 = 1 + [\eta]C_p$ is the linear viscosity of the polymer solution. It is seen from Figure 3 that the measured $v_c(\phi_c,C_p)\cdot \eta_c(C_p)/[v_c(0^+,0)\eta_0]$ in the polymer solution decays slower than that in the pure colloidal suspension. For a given ϕ_c, the measured $v_c(\phi_c,C_p)\ \eta_c(C_p)/[v_c(0^+,0)\eta_0]$ increases with C_p. At the high colloid concentrations, the increase is more than 100%. To separate the effect of the thermodynamic interaction (i.e., the depletion attraction) from that of the hydrodynamic interaction, we define the ratio

$$\beta_1(\phi_c,C_p) = \frac{v_c(\phi_c,C_p)\ \eta_c(C_p)}{v_c(\phi_c,0)\eta_0} \simeq [1 - (R_h/R_s)^3\phi_c]^{K_p} \simeq 1 - K_p(R_h/R_s)^3\phi_c \quad (16)$$

Equation 16 states that $\beta_1(\phi_c,C_p)$ is a linear function of ϕ_c, and its slope depends on K_p in eq 10 ($K_p < 0$).

Figure 4 shows the plots of $\beta_1(\phi_c,C_p)$ as a function ϕ_c for the mixture samples with three different polymer concentrations. The data can be well-described by a linear function (the solid lines), when the colloid concentration is small ($\phi_c < 0.1$). The deviation from the linear behavior can be attributed to the non-hard-sphere hydrodynamics at higher ϕ_c, as discussed in the above. We notice that the fitted solid lines in Figure 4 have the form

$$\beta_1(\phi_c,C_p) = \frac{1 - K_p(R_h/R_s)^3\phi_c}{1 - K_p(R_h/R_s)^3 0.014} \simeq 1 - K_p(R_h/R_s)^3(\phi_c - 0.014) \quad (17)$$

Table 1. Sedimentation Results from the Colloid−PEP Mixture Samples[a]

sample no.	ϕ_c	C_p (g/cm^3)	C_p/C^*	β_1	K_p
1	0.146	0.0042	0.24	1.18	−0.62
2	0.146	0.0097	0.54	1.44	−1.52
3	0.146	0.0178	0.99	1.80	−2.76
4	0.146	0.0260	1.45	2.26	−4.34
5	0.087	0.0081	0.46	1.27	−1.68
6	0.087	0.0172	0.96	1.48	−2.99
7	0.087	0.0247	1.37	1.60	−3.74
8	0.087	0.0396	2.20	1.82	−5.11
9	0.041	0.0077	0.43	1.09	−1.52
10	0.041	0.0159	0.88	1.18	−3.03
11	0.041	0.0227	1.26	1.22	−3.71
12	0.041	0.0364	2.02	1.30	−5.06
13	0.041	0.0473	2.62	1.35	−5.90

[a] K_p is obtained using the equation $K_p = (1 - \beta_1)/[(1.3)^3(\phi_c - 0.014)]$.

which has a slightly different intercept from that of eq 16. This difference reflects the fact that there is no depletion effect observed in the dilute sample with $\phi_c = 0.014$. A similar expansion can also be made for the velocity ratio

$$\beta_2(\phi_c,C_p) = \frac{v_c(\phi_c,0)}{v_c(\phi_c,C_p)} \simeq \frac{1 + [\eta]C_p}{1 - K_p(R_h/R_s)^3(\phi_c - 0.014)} \quad (18)$$

As shown in Figure 1, the measured $\beta_2(\phi_c,C_p)$ is a linear function of C_p and its slope decreases with increasing ϕ_c. The data in Figure 1 thus is in good agreement with eq 18.

From the slope of the linear fits in Figure 4, one can obtain K_p for the corresponding mixture samples. The slope method, however, requires a systematic measurement of $\beta_1(\phi_c,C_p)$ as a function of ϕ_c. Another way to obtain K_p is to convert each individually measured $\beta_1(\phi_c,C_p)$ to K_p by using eq 17. In this way, we obtain K_p for each mixture sample with different colloid and polymer concentrations. The final results are summarized in Table 1. Figure 5 shows the measured K_p as a function of the polymer volume fraction $\phi_p \equiv C_p/C^*$ for the mixture samples with $\phi_c = 0.041$ (triangles), 0.087 (diamonds), and 0.146 (squares). The solid curve in Figure 5, is the calculated K_p using eq 10. The equation contains two interaction parameters, the amplitude $\tilde{P}(\phi_p)$ and the range λ; both of them have been measured in a recent neutron scattering experiment.[9,10] In the plot we use the measured value of $\lambda = 2.9$, which is very close to the calculated value $\lambda = 1 +$

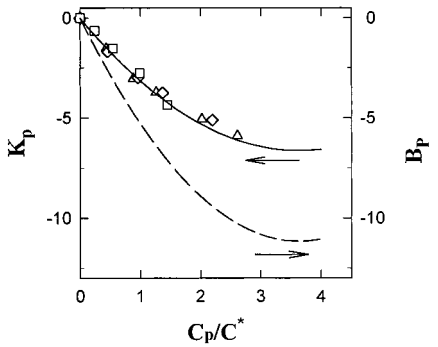

Figure 5. Measured K_p as a function of the polymer volume fraction C_p/C^* for the mixture samples with $\phi_c = 0.041$ (triangles), 0.087 (diamonds), and 0.146 (squares). The solid curve is the calculated K_p using eq 10, and the dashed curve shows B_p in eq 13.

$R_g/R_m = 3.07$. The measured $\tilde{P}(\phi_p)$ has the form $\tilde{P} = -0.054 + 0.178(\phi_p/\alpha) - 0.0245(\phi_p/\alpha)^2$, where $\alpha = V_f/V$ is the ratio the free volume V_f not occupied by the colloidal particles and their surrounding depletion zones to the sample volume V. It has been shown[10,20] that the depletion interaction in the colloid−polymer mixtures should be described by the effective polymer volume fraction ϕ_p/α instead of ϕ_p. However, we find from the sedimentation measurements that K_p is insensitive to ϕ_c [and hence is insensitive to $\alpha(\phi_c)$]. As shown in Figure 5, the measured K_p for different colloid concentrations collapses on to a single master curve. Therefore, we take $\alpha(\phi_c) = 1$ for the amplitude $\tilde{P}(\phi_p)$ in eq 10.

The measured $\tilde{P}(\phi_p)$ consists of three terms.[9,10] The small negative intercept represents a weak repulsive interaction between the soft surfactant shells of the particles. The linear coefficient describes the depletion attraction induced by the noninteracting polymer chains (an ideal gas). The reduction of the depletion attraction at higher polymer concentrations (due to the quadratic term in $\tilde{P}$) can be explained by the screening of the polymer chain−chain interaction in the semidilute regime. It has been shown in Figure 2 that the pure colloidal suspension can be adequately described by the hard-sphere hydrodynamics, once R_h is used to determine the colloid volume fraction. Because R_h is larger than the particle interaction radius R_s, the short-range thermodynamic interaction between the particles is washed out during sedimentation. Therefore, we drop the constant term in the measured $\tilde{P}(\phi_p)$ and take $\tilde{P}(\phi_p) = 0.178\phi_p - 0.0245\phi_p^2$ to calculate K_p, which is shown by the solid curve in Figure 5. Note that there are not any adjustable parameters for the calculated K_p and the agreement between the measurement and the theory is excellent. As mentioned in section 2, K_p plays a role similar to that of parameter B_p in thermodynamics. By comparing eq 10 with eq 13, we find that both K_p and B_p are proportional to $\tilde{P}(\phi_p)$, but the proportionality constant is different and changes with the range parameter λ. This is because K_p and B_p are obtained with different weighting factors. Using $\lambda = 2.9$ we find $K_p = -20.5\tilde{P}(\phi_p)$ and $B_p = -34.5\tilde{P}(\phi_p)$. To compare K_p with B_p numerically, we also plot B_p in Figure 5 (the dashed curve).

5. Conclusion

We have studied sedimentation of the concentrated colloidal particles through a nonadsorbing polymer solution. The colloidal particles used are sterically stabilized $CaCO_3$ nanoparticles, and the polymer is hydrogenated polyisoprene. The thermodynamic properties of the colloid−polymer system have been well-characterized recently using the small-angle neutron scattering technique.[9,10,19] In the experiment, we measured the particle sedimentation velocity $v_c(\phi_c,C_p)$ as a function of the colloid volume fraction ϕ_c and the polymer concentration C_p. The measured $v_c(\phi_c,0)$ for the pure colloidal samples is found to be adequately described by the hard-sphere hydrodynamics, once the particle's hydrodynamic radius R_h is used to determine the colloid volume fraction. When the polymer is added into the colloidal suspension, the measured $v_c(\phi_c,C_p)$ is found to increase with C_p. At high colloid concentrations, the increase is as much as 100%. The measurements thus reveal a large effect of the depletion interaction on colloidal sedimentation. With a simple normalization scheme, we obtain a parameter K_p to describe the effect of the depletion attraction on particle sedimentation. The measured K_p is found to be in excellent agreement with the theoretical calculation based on the known interaction parameters obtained from the scattering measurements. The experiment, therefore, confirms the theoretical prediction for the effect of the thermodynamic interaction on particle sedimentation.

The experiment reveals several interesting features of colloidal sedimentation in semidilute polymer solutions. First, the sedimentation measurements clearly demonstrate their sensitivity to the thermodynamic interaction between the particles. In the concentrated colloid−polymer mixtures, the polymer-induced depletion interaction is found to be very effective in controlling the particle sedimentation. Second, the sedimentation velocity $v_c(\phi_c,C_p)$ is more sensitive to the long-range thermodynamic interaction compared with the short-range interactions. For the colloid−PEP mixtures used in the experiment, the range of the depletion interaction is controlled by the polymer radius of gyration R_g, which is comparable to R_h. Finally, the parameter K_p, which describes the effect of the thermodynamic interaction on particle sedimentation, plays a role similar to that of the virial coefficient B_p in thermodynamics. Colloidal sedimentation, therefore, becomes a useful tool for measuring the thermodynamic interaction between the particles. The experiment demonstrates the effectiveness of using the sedimentation method to study interaction-related phenomena in different colloidal suspensions.

Acknowledgment. We have benefited from a fruitful collaboration with Bruce J. Ackerson. We would also like to thank M. Lucas for making the centrifuge cells. This work was supported by the National Aeronautics and Space Administration under Grant No. NAG3-1852.

References and Notes

(1) Wirtz, D. *Phys. Rev. Lett.* **1995**, *75*, 2436.
(2) de Gennes, P.-G. *Scaling Concepts in Polymer Physics*; Cornell University Press: Ithaca, NY, 1979; p 80.
(3) Russel, W. B.; Saville, D. A.; Schowalter, W. R. *Colloidal Dispersions*; Cambridge University Press: Cambridge, U.K., 1989; p 394.
(4) Phillies, G. D. J. *J. Phys. Chem.* **1989**, *93*, 5029. Phillies, G. D. J.; Clomenil, D. *Macromolecules* **1993**, *26*, 167.
(5) Asakura, S.; Oosawa, F. *J. Chem. Phys.* **1954**, *22*, 1255.
(6) Vrij, A. *Pure Appl. Chem.* **1976**, *48*, 471.
(7) Tong, P.; Ye, X.; Ackerson, B. J.; Fetters, L. J. *Phys. Rev. Lett.* **1997**, *79*, 2363.

(8) Langevin, D.; Rondelez, F. *Polymer* **1978**, *19*, 875.
(9) Ye, X.; Narayanan, T.; Tong, P.; Huang, J. S. *Phys. Rev. Lett.* **1996**, *76*, 4640.
(10) Ye, X.; Narayanan, T.; Tong, P.; Huang, J. S.; Lin, M. Y.; Carvalho, B. L.; Fetters, L. J. *Phys. Rev. E* **1996**, *54*, 6500.
(11) Davis, R. H.; Acrivos, A. *Annu. Rev. Fluid Mech.* **1985**, *17*, 91.
(12) Batchelor, G. K. *J. Fluid Mech.* **1972**, *52*, 245.
(13) Newman, J.; Swinney, H. L.; Berkowitz, S.; Day, L. A. *Biochemistry* **1974**, *13*, 4832.
(14) Kops-Werkhoven, M. M.; Pathmamanoharon, C.; Vrij, A.; Fijnaut, H. M. *J. Chem. Phys.* **1982**, *77*, 5913.
(15) Tong, P.; Witten, T. A.; Huang, J. S.; Fetters, L. J. *J. Phys.* (*Paris*) **1990**, *51*, 2813.
(16) Mays, J.; Hadjichristidis, N.; Fetters, L. *Macromolecules* **1984**, *17*, 2723.
(17) Mays, J.; Fetters, L. *Macromolecules* **1989**, *22*, 921.
(18) Davidson, N. S.; Fetters, L. J.; Funk, W. G.; Hadjichristidis, N.; Graessley, W. W. *Macromolecules* **1987**, *20*, 2614.
(19) Ye, X.; Tong, P.; Fetters, L. J. *Macromolecules* **1997**, *30*, 4103.
(20) Ilett, S. M.; Orrock, A.; Poon, W.; Pusey, P. N. *Phys. Rev. E* **1995**, *51*, 1344.

MA971892Z